Neuron, Vol. 35, 147–159, July 3, 2002, Copyright ©2002 by Cell Press

Quantal Release of Glutamate Generates Pure Kainate and Mixed AMPA/Kainate EPSCs in Hippocampal Neurons

Rosa Cossart,[2] Jérôme Epsztein,[2] Roman Tyzio, Hélène Becq, June Hirsch, Yehezkel Ben-Ari,[1] and Valérie Crépel
INMED-INSERM U.29 and
Université de La Méditerranée
Parc scientifique de Luminy
BP 13
13273 Marseille Cedex 9
France

Summary

The relative contribution of kainate receptors to ongoing glutamatergic activity is at present unknown. We report the presence of spontaneous, miniature, and minimal stimulation-evoked excitatory postsynaptic currents (EPSCs) that are mediated solely by kainate receptors ($EPSC_{kainate}$) or by both AMPA and kainate receptors ($EPSC_{AMPA/kainate}$). $EPSC_{kainate}$ and $EPSC_{AMPA/kainate}$ are selectively enriched in CA1 interneurons and mossy fibers synapses of CA3 pyramidal neurons, respectively. In CA1 interneurons, the decay time constant of $EPSC_{kainate}$ (circa 10 ms) is comparable to values obtained in heterologous expression systems. In both hippocampal neurons, the quantal release of glutamate generates kainate receptor-mediated EPSCs that provide as much as half of the total glutamatergic current. Kainate receptors are, therefore, key players of the ongoing glutamatergic transmission in the hippocampus.

Introduction

There are three main types of glutamatergic ionotropic receptors: NMDA, AMPA, and kainate receptors. In contrast to AMPA and NMDA receptors (and despite their widespread expression throughout the brain), little is known about the properties of kainate receptors containing synapses in adult central neurons and the contribution of kainate receptors to the ongoing synaptic transmission. With the development of selective antagonists that block AMPA, but not kainate receptors (Paternain et al., 1995; Wilding and Huettner, 1995), excitatory postsynaptic currents (EPSCs) with a kainate receptor-mediated component have been identified in the hippocampus (Ben Ari and Cossart, 2000; Bureau et al., 1999; Castillo et al., 1997; Cossart et al., 1998; Frerking et al., 1998; Vignes and Collingridge, 1997), the amygdala (Li and Rogawski, 1998), the cerebellum (Bureau et al., 2000), the spinal cord (Li et al., 1999), the retina (DeVries, 2000), and in the immature neocortex (Kidd and Isaac, 1999). In most of these studies, bulk stimulation of synaptic inputs evoked a mixed AMPA/kainate receptor-mediated EPSC with a large AMPA component and a small kainate one. In addition, whereas a single stimulus readily evoked the AMPA component of the EPSCs, the kainate component required repetitive and/or strong stimulations. This has led to the suggestion that kainate receptors may be located extrasynaptically, as they are only activated when large amounts of glutamate are released (see Frerking and Nicoll, 2000, and Lerma et al., 2001, for a review). Another problem is the discrepancy between the decay time constant of bulk stimulation-evoked kainate receptor-mediated EPSCs and the rapid kinetics of currents generated by homomeric kainate receptors expressed in heterologous expression cells (ibid). This has lead to the suggestion that in vivo, either there is a complex subunit composition of kainate receptors or that special mechanisms regulate the kinetics of the current (ibid). Taken altogether, these studies suggest that glutamatergic synaptic transmission is entirely mediated by AMPA receptors (and NMDA receptors when the Mg^{2+} block is alleviated), with the contribution of kainate receptors being restricted to special conditions in which hyperactivity leads to enhanced glutamate release (such as seizures that have been classically associated with kainate receptor activation) (Ben Ari and Cossart, 2000). If kainate receptors participate in ongoing glutamatergic transmission, then the quantal release of glutamate will generate spontaneous and miniature EPSCs mediated by kainate receptors ($EPSC_{kainate}$). The study of these events will give an indication on the contribution of kainate receptors to ongoing synaptic transmission and an estimation of the genuine kinetics of $EPSC_{kainate}$. Indeed, when many axons are activated by bulk stimulation or repetitive stimuli, the kinetics of EPSCs may be affected by different processes, including desensitization of receptors and summation of individual events.

In the present study, we report the presence of TTX-resistant miniature EPSCs generated by the activation of kainate receptors by the quantal release of glutamate. These EPSCs are of two types in mature hippocampal neurons: pure $EPSC_{kainate}$ generated in synapses that possess kainate, but not AMPA, receptors and mixed $EPSC_{AMPA/kainate}$ generated in synapses endowed of both types of receptors. Most interestingly, these EPSCs have a preferential distribution in the hippocampus: pure $EPSC_{kainate}$ are enriched in CA1 interneurons and mixed $EPSC_{AMPA/kainate}$ in CA3 pyramidal neurons at mossy fiber synapses. In contrast, only pure $EPSC_{AMPA}$ are generated in CA1 pyramidal neurons that do not express functional postsynaptic kainate receptors (Bureau et al., 1999). The kinetics of pure $EPSC_{kainate}$ in CA1 interneurons–albeit slower than the $EPSC_{AMPA}$–are much faster than those reported with bulk stimulations of afferent fibers and are compatible with values obtained in heterologous expression systems. To estimate the relative contribution of AMPA and kainate receptors to the tonic glutamatergic transmission, we have performed a quantitative estimation of the total current mediated by kainate receptors. Our observations show that kainate receptors are key players of the ongoing ionotropic glutamatergic transmission in the hippocampus.

[1]Correspondence: ben-ari@inmed.univ-mrs.fr
[2]These authors contributed equally to this work.

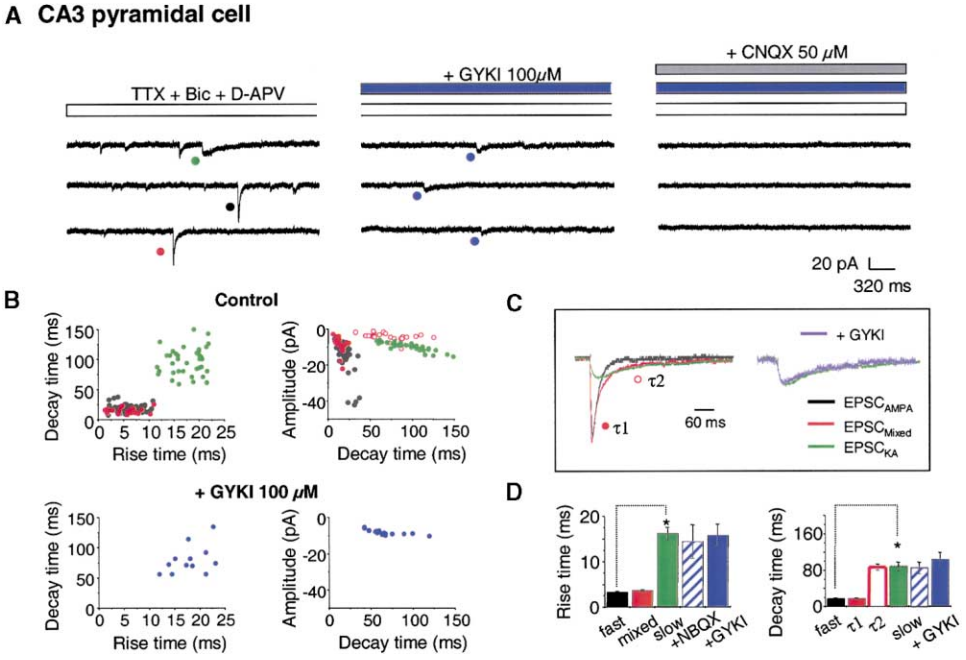

Figure 1. $EPSCs_{kainate}$ Can Be Isolated from mEPSCs Based on Their Pharmacological and Kinetic Profile in CA3 Pyramidal Cells

(A) Miniature EPSCs recordings in the presence of TTX (1 μM), bicuculline (10 μM), and D-APV (50 μM) from a representative CA3 pyramidal cell, show that $mEPSC_{kainate}$ (closed purple circle) can be isolated pharmacologically when GYKI 52466 (100 μM) is added to the saline and blocked by CNQX (50 μM) ; Vh: −60 mV. Note that in control conditions in the CA3 pyramidal cell, three types of mEPSCs can be distinguished based on the time course of their decay: fast (closed black circle), slow (closed green circle), and mixed EPSCs with a double decaying phase (closed red circle). Traces are nonconsecutives.

(B) Scatter plots of the rise time constant (left column) or amplitude (right column) versus the decay time constant were calculated in 157 mEPSCs and recorded from a CA3 pyramidal cell in the absence (top) or in the presence of GYKI (100 μM, bottom). Note that two families of events are clustered in separate areas of the graph, with the fast (closed black circle) and the slow events (closed green circle) having no significant correlation between rise and decay times within the two groups ($r = 0.06$ and 0.14, respectively). The decay time constant versus amplitude distributions obtained when plotting the first (closed red circle) and the second (open red circle) components of mixed events overlapped that of the fast (closed black circle) and slow event (closed green circle) families, respectively. In the presence of GYKI, only events with a slow time course and a small amplitude (closed purple circle) remain.

(C) Superimpositions of the digitally averaged traces of fast (black), mixed (red), and slow (green) mEPSCs and GYKI-resistant mEPSCs (purple). Note that slow events, the second component of mixed events, and GYKI-resistant events have the same time course.

(D) Bar graph of averaged values of rise times (left) and decay times (right) show that the time course of slow events, GYKI or NBQX (1 μM)-resistant events, and the second component of mixed events (tau 2) are identical ($p > 0.5$) but different from that of fast events (*$p < 0.05$; $n = 25$, eight and six cells for control, GYKI and NBQX experiments, respectively).

Results

Three Populations of Glutamatergic Miniature EPSCs in CA3 Pyramidal Cells and CA1 Interneurons

Whole-cell recordings of glutamatergic miniature activity were obtained from a total of 36 CA3 pyramidal cells and 26 CA1 stratum oriens interneurons. A majority of CA1 interneurons ($n = 7$ out of 15 identified cells) recorded in stratum oriens corresponded to the previously described O-LM cells (oriens lacunosum moleculare interneurons) (Katona et al., 1999). Cells were filled with biocytin and morphologically identified post hoc. Miniature excitatory postsynaptic currents (mEPSCs) were recorded in the presence of the sodium channel blocker TTX (1 μM), the $GABA_A$ receptor antagonist bicuculline (10 μM), and the NMDA receptor antagonist D-APV (50 μM). Visual inspection of the kinetics of mEPSCs revealed three types of events in both CA3 pyramidal neurons and CA1 interneurons: fast, slow, and mixed events. The three populations of events were mediated by non-NMDA receptors, as they were blocked by the AMPA/kainate receptor antagonist CNQX (50 μM; Figures 1A and 2A). The plot of mEPSCs decay times versus 10%–90% rise times revealed the presence of slow ($mEPSC_{slow}$) and fast ($mEPSC_{fast}$) events that clustered within two separate areas of the graph (Figures 1B and 2B). A third group of events ($mEPSC_{mixed}$) had a double exponential decay with the early and late decay time constants identical to those of the fast and slow monoexponential EPSCs, respectively (Table 1; Figures 1D and 2D). Interestingly, the distribution of the amplitude versus decay time of the two components of $EPSC_{mixed}$ overlapped that of the $mEPSC_{fast}$ and $mEPSC_{slow}$ (Figures 1B and 2B), suggesting that mixed events were the summation of fast and slow events. Bath applications of the selective AMPA receptor antagonist GYKI 52466 (100 μM) blocked the fast events, indicating that they were mediated by AMPA receptors (i.e., $mEPSC_{fast} = mEPSC_{AMPA}$). Only slow mEPSCs were observed in the presence of GYKI 52466 (100 μM; Figures 1A and 2A), but their frequency was reduced to 59.4% ± 18.2% of control in pyramidal cells ($n = 8$) and to 54% ± 20% of

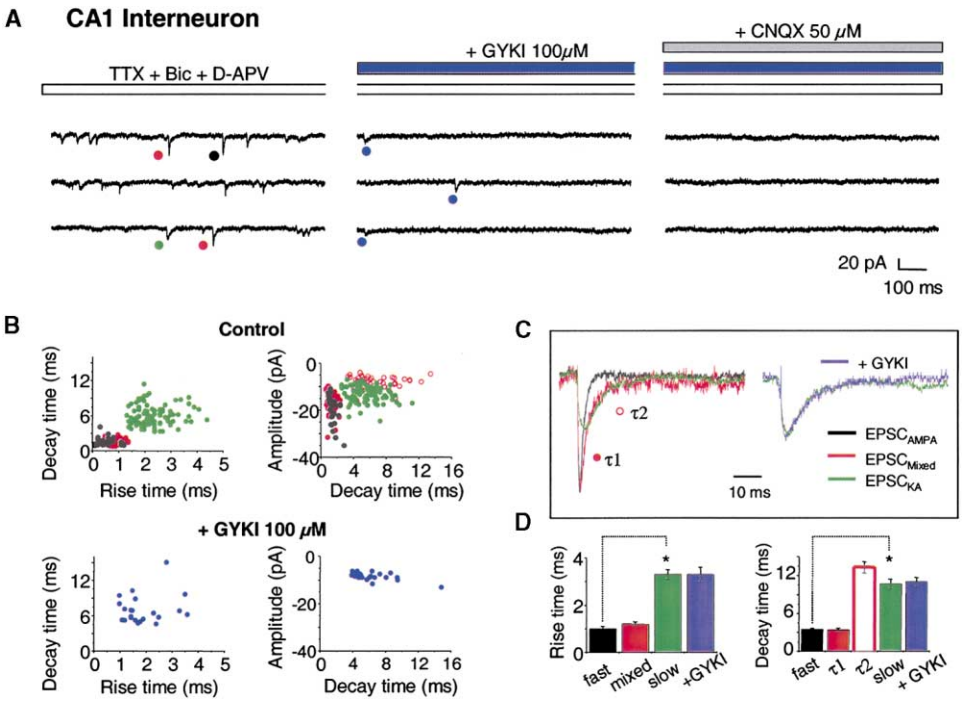

Figure 2. $EPSC_{kainate}$ Can Be Isolated from mEPSCs Based on Their Pharmacological and Kinetic Profile in CA1 Interneurons

(A) Miniature EPSCs recordings in the presence of TTX (1 μM), bicuculline (10 μM), and D-APV (50 μM) from a representative CA1 stratum oriens interneuron show that $mEPSC_{kainate}$ (closed purple circle) can be isolated pharmacologically when GYKI 52466 (100μM) is added to the saline and blocked by CNQX (50 μM); Vh: −60 mV. Note that in control conditions in the CA1 interneuron, three types of mEPSCs can be distinguished based on the time course of their decay: fast (closed black circle), slow (closed green circle), and mixed EPSCs with a double decaying phase (closed red circle). Traces are nonconsecutives.

(B) Scatter plots of the rise time constant (left column) or amplitude (right column) versus decay time constant are shown, calculated in 110 mEPSCs recorded from a CA1 stratum oriens interneuron in the absence (top) or presence of GYKI (100 μM, bottom). Note that two families of events are clustered in separate areas of the graph, the fast (closed black circle) and slow events (closed green circle), with no significant correlation between rise times and decays within the two groups ($r = 0.1$ and 0.14, respectively). The decay time constant versus amplitude distributions obtained when plotting the first (closed red circle) and the second (open red circle) components of mixed events overlapped that of the fast (closed black circle) and slow event (closed green circle) families, respectively. In the presence of GYKI, only events with a slow time course and a small amplitude (closed purple circle) remain.

(C) Superimpositions of the digitally averaged traces of fast (black), mixed (red), and slow (green) mEPSCs and of GYKI-resistant mEPSCs (purple) are illustrated. Note that slow events, the second component of mixed events, and GYKI-resistant events have the same time course.

(D) Bar graph of averaged values of rise times (left) and decay times (right) show that the time course of slow events, GYKI-resistant events, and the second component of mixed events (tau 2) are identical ($p > 0.5$) but different from that of fast events (15 and 10 cells for control and GYKI experiments, respectively; $^*p < 0.05$).

control in interneurones ($n = 10$). Only slow events were also observed in the presence of GYKI 53655 (30 μM, $n = 3$ in CA3 pyramidal cells and CA1 interneurons) or a low concentration of NBQX (1 μM, $n = 6$ in CA3 pyramidal cells and CA1 interneurons; data not shown) that also preferentially block AMPA receptors (Bureau et al., 1999). Slow mEPSCs recorded in the presence of GYKI (52466 or 53655) or NBQX were fully blocked by the AMPA/kainate receptor antagonist CNQX (50 μM), indicating that they were mediated by kainate receptors ($mEPSC_{kainate}$, r: 16.3 ± 2.7 ms and τ: 98 ± 17 ms, $n = 8$ for CA3 pyramidal cells; r: 3.3 ± 0.3 ms and τ: 11.1 ± 0.1 ms, $n = 10$ for CA1 interneurons). Miniature $EPSC_{slow}$ and $mEPSC_{kainate}$ represented the same population of events since (1) the group of events obtained when plotting $EPSC_{kainate}$ overlapped that of $EPSC_{slow}$, but not that of $EPSC_{fast}$ (Figures 1B and 2B). (2) They had similar digitally obtained averages (Figures 1C and 2C). (3) They had similar rise and decay time values (Figures 1D and 2D; Table 1; chisquare >0.5).

GYKI (52466 or 53655) and NBQX also blocked mixed mEPSCs, suggesting that AMPA receptors contributed to their generation. In order to determine whether the slow component of the mixed mEPSCs was mediated by the activation of kainate receptors, we used a pharmacological agent, SYM 2081 (10μM), that selectively desensitizes kainate receptors (Li et al. 1999; DeVries, 2000). In the presence of SYM 2081, only AMPA receptor-mediated events were recorded in CA3 pyramidal cells and CA1 interneurons (Figure 3), since all the SYM-resistant events were blocked by GYKI 52466 (100 μM) or NBQX (1 μM). In CA3 pyramidal cells and CA1 interneurons, the mean kinetics of the AMPA receptor-mediated events recorded in the presence of SYM 2081 (r: 2.1 ± 0.26 ms and τ: 11.7 ± 2.3 ms, $n = 6$ in CA3 pyramidal cells; r: 0.72 ± 0.1 ms and τ: 3.6 ± 0.54 ms, $n = 5$ in CA1 interneurons) were not significantly different from those of the fast events recorded in control conditions (r: 2.8 ± 0.45 ms and τ: 15.6 ± 2.7 ms, $n = 6$ in CA3 pyramidal cells; r: 0.9 ± 0.19 ms and τ: 3.6 ± 0.19

Table 1. Kinetics Properties of $EPSC_{AMPA}$, $EPSC_{KA}$, and $EPSC_{AMPA/KA}$ in Three Hippocampal Cell Types

Cell Type	Event Type	sEPSCs	mEPSCs	eEPSC
CA3 Pyramidal cells				
	$EPSC_{AMPA}$	r: 3.5 ± 0.5 ms τ: 21.8 ± 2.2 ms A: 16.4 ± 1.6 pA (n = 6)	r: 3.4 ± 0.22 ms τ: 17.6 ± 1.3 ms A: 14 ± 1.5 pA (n = 25)	–
	$EPSC_{KA}$	r: 12.6 ± 0.8 ms τ: 91.3 ± 11.4 ms A: 9.1 ± 1.2 pA (n = 6)	r: 15.8 ± 1.4 ms τ: 92 ± 10 ms A: 8.5 ± 0.7 pA (n = 25)	–
	$EPSC_{AMPA/KA}$	r: 3.7 ± 0.5 ms τ1: 18.8 ± 2.8 ms A1: 20 ± 4 pA τ2: 94 ± 13.8 ms A2: 9.6 ± 2.5 pA (n = 6)	r: 3.6 ± 0.19 ms τ1: 17.6 ± 1.2 ms A1: 9.8 ± 0.9 pA τ2: 87.3 ± 6.5 ms A2: 4.6 ± 0.5 pA (n = 25)	r: 3.2 ± 0.2 ms τ1: 10.3 ± 0.8 ms A1: 38.3 ± 13.3 pA τ2: 48 ± 2 ms A2: 18.9 ± 7 pA (n = 5)
CA1 Interneurons				
	$EPSC_{AMPA}$	r: 0.7 ± 0.1 ms τ: 2.7 ± 0.3 ms A: 25.4 ± 7.8 pA (n = 5)	r: 1 ± 0.1 ms τ: 2.7 ± 0.3 ms A: 17 ± 2.4 pA (n = 10)	r: 0.9 ± 0.2 ms τ: 3.8 ± 0.4 ms A: 14.7 ± 1.4 pA (n = 6)
	$EPSC_{KA}$	r; 2.7 ± 0.6 ms τ: 11.3 ± 0.9 ms A: 15.6 ± 3.2 pA (n = 5)	r: 3.3 ± 0.2 ms τ: 10.7 ± 0.7 ms A: 9.6 ± 1.6 pA (n = 15)	r: 3.8 ± 0.4 ms τ: 16 ± 4 ms A: 5.4 ± 0.7 pA (n = 4)
	$EPSC_{AMPA/KA}$	r: 0.9 ± 0.1 ms τ1: 2.5 ± 0.2 ms A1: 27.2 ± 9 pA (n = 5) τ2: 11.3 ± 0.9 ms A2: 12.5 ± 3.3 pA (n = 5)	r: 1.2 ± 0.1 ms τ1: 2.5 ± 0.2 ms A1: 11.0 ± 1.7 pA τ: 13.3 ± 0.9 ms A2: 7.9 ± 2.2 pA (n = 15)	–
CA1 Pyramidal cells				
	$EPSC_{AMPA}$	r: 2.8 ± 0.3 ms τ: 11.6 ± 1.4 ms A: 11 ± 1.8 pA (n = 8)	–	–

Abbreviations: A, amplitude; A1, amplitude of the first component of the mixed event; A2, amplitude of the second component of the mixed event; r, rise time; τ, decay time constant; τ1, decay time constant of the first component of the mixed event; τ2, decay time constant of the second component of the mixed event.

ms, n = 5 in CA1 interneurons, $p > 0.05$). In addition, in the presence of SYM 2081, we did not observe any significant change in the frequency of the $EPSC_{AMPA}$, as compared with the fast events recorded in control conditions (the frequency was 0.2 ± 0.06 Hz in control conditions and 0.31 ± 0.1 Hz in SYM 2081 in six CA3 pyramidal cells; 0.2 ± 0.07 Hz in control conditions and 0.25 ± 0.07 Hz in SYM 2081 in five CA1 interneurons, $p > 0.05$). Miniature $EPSC_{mixed}$ were not recorded in the presence of SYM, indicating that in addition to AMPA receptors, kainate receptors also contributed to their generation ($EPSC_{mixed} = EPSC_{AMPA/kainate}$). This experiment also confirmed that $EPSC_{slow}$ were mediated by kainate receptors.

The plots of rise times versus decay times and decay times versus amplitudes obtained for the SYM-resistant events revealed a homogeneous group of events that overlapped that of the $mEPSC_{fast}$ and not that of the $mEPSC_{slow}$ recorded in the absence of SYM (Figure 3). Thus, all AMPA receptor-mediated events (i.e., filtered and nonfiltered) are included in the fast events population ($EPSC_{AMPA}$) and have rapid kinetic properties that differ from the population of slow events mediated by kainate receptors.

Therefore, the quantal release of glutamate activates kainate receptors in both CA3 pyramidal neurons and CA1 interneurons. Glutamatergic events are either pure AMPA or pure kainate receptor-mediated or mixed with both AMPA and kainate receptors participating to their generation. We next determined if electrical activation of glutamatergic inputs could evoke similar EPSCs in physiological conditions (i.e., in the absence of TTX). We used minimal stimulation to activate single fibers.

Minimal Stimulations Evoke Both Pure $mEPSC_{kainate}$ and Mixed $mEPSC_{AMPA/kainate}$

Minimal stimulations were performed in the presence of bicuculline and D-APV. In these experiments, the concentration of divalent cations was increased in the perfusion saline (4 mM Ca^{2+} and 6 mM Mg^{2+}) in order to reduce the level of spontaneous activity and prevent the generation of epileptiform events by bicuculline.

In CA3 pyramidal cells, minimal stimulations of stratum lucidum principally evoked an unitary EPSC with a fall best fitted by a double exponential (Figure 4A; other events were fast, mono decaying EPSCs). Their decay was within the same range as that obtained in mixed mEPSCs (Table 1, Figure 4C). NBQX (1 μM) selectively blocked the fast component of the evoked EPSCs (n = 5, Figure 4A), and the slow component was blocked by CNQX (50 μM). Therefore, minimal stimulation of glutamatergic afferents evoked a unitary mixed $EPSC_{AMPA/kainate}$ in CA3 pyramidal cells. The amplitudes of the AMPA and kainate components of the unitary mixed $EPSC_{AMPA/kainate}$ were strongly correlated ($r > 0.85$ for all plots, n = 5; Figure 4B), indicating a coordinated activation of AMPA and kainate receptors by different amounts of glutamate released within the same synaptic cleft (McAllister and Stevens, 2000; Watt et al., 2000).

A similar paradigm could generate pure $mEPSC_{kainate}$ in CA1 interneurons. Minimal stimulation of stratum oriens generated either a pure unitary AMPA receptor-medi-

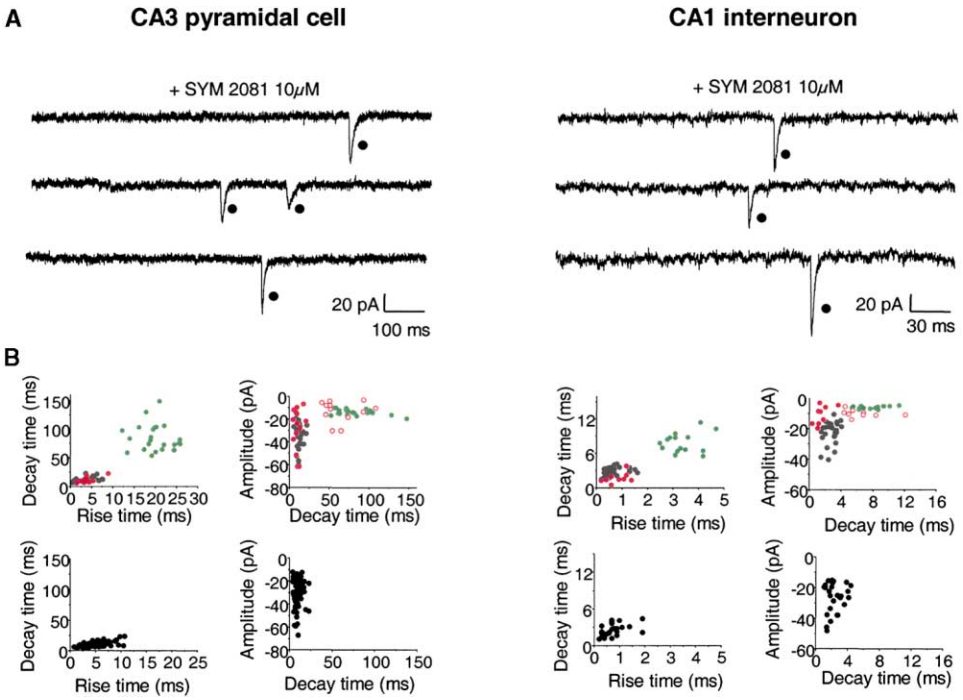

Figure 3. An Antagonist for Kainate Receptors (SYM 2081) Abolishes $mEPSC_{kainate}$ and $mEPSC_{mixed}$

(A) Recordings of miniature EPSCs recordings, in the presence of TTX (1 μM), bicuculline (10 μM), and D-APV (50 μM) from a representative CA3 pyramidal cell (left) and a CA1 interneuron (right) show that $mEPSC_{AMPA}$ (closed black circle) can be isolated pharmacologically when SYM 2081 (10 μM) is added to the saline; Vh: −60 mV. Traces are nonconsecutives.

(B) Scatter plots of the rise time constant (left column) or amplitude (right column) versus decay time constant calculated in mEPSCs recorded from a CA3 pyramidal cell or a CA1 interneuron are shown in the absence (top) or in the presence of SYM 2081 (10μM, bottom). Note that in control conditions, two families of events are clustered in separate areas of the graph, the fast (closed black circle) and the slow events (closed green circle). The decay time constant versus amplitude distributions obtained when plotting the first (closed red circle) and the second (open red circle) components of mixed events overlapped that of the fast (closed black circle) and slow event (closed green circle) families, respectively. In the presence of SYM 2081, only fast events (closed black circle) remain.

ated event or a pure slow EPSC (Figure 5A) with the same kinetics as the $mEPSC_{kainate}$ (Table 1, Figure 5B). This slow EPSC was mediated by the activation of kainate receptors since it was NBQX-resistant (1 μM) and blocked by CNQX (50 μM) ($n = 4$, Figure 5A). Therefore, the stimulation of single glutamatergic afferents on interneurons can generate evoked currents that are exclusively mediated by kainate receptors.

Estimation of the Contribution of Kainate Receptors to Miniature Glutamatergic Activity in the Hippocampus

To estimate the total contribution of kainate receptor activation to glutamatergic miniature activity in hippocampal slices, we calculated the frequency of $mEPSC_{AMPA}$, $mEPSC_{kainate}$, and $mEPSC_{AMPA/kainate}$ in CA3 pyramidal cells and CA1 interneurons. To obtain a physiologically relevant estimation, the experiments were performed in the absence of AMPA and kainate receptor antagonists. We relied on the kinetics of the $EPSC_{AMPA}$ and $EPSC_{kainate}$ to perform this task (see Experimental Procedures). $EPSC_{AMPA/kainate}$ were identified by the fact that their decay time constant was best fitted by a double exponential function. Our results show that the contribution of kainate receptors differs in CA1 interneurons and in CA3 pyramidal cells. Interneurons predominantly generated pure $EPSC_{kainate}$ that represented almost half of the total number of events (46% ± 2%, $n = 11$). In contrast, in CA3 pyramidal cells, kainate receptors were mostly involved in mixed EPSCs, which represented 34.2% ± 5.3% ($n = 25$) of the total activity. These observations showed that in the hippocampus, a high percentage of glutamatergic events are mediated by kainate receptors. Both types are absent from CA1 pyramidal neurons, which do not express functional postsynaptic kainate receptors (Bureau et al., 1999; $n = 8$; data not shown).

We extended this analysis by calculating the mean percent of charge carried by kainate receptors in digitally averaged $mEPSC_{AMPA/kainate}$ and $mEPSC_{kainate}$ versus the total charge carried by AMPA and kainate receptors in mEPSCs (Figure 6 and see Experimental Procedures). The mean charge transferred through kainate receptors was greater than that through AMPA receptors in CA3 pyramidal cells (73% ± 2% of the total charge, $n = 25$) and CA1 interneurons (60% ± 1.8%, $n = 10$). Taking into account the frequency of each type of events and the charge transferred through AMPA or kainate receptors, we could estimate the proportion of current carried by kainate receptors. These results show that kainate receptors are major postsynaptic mediators of miniature glutamatergic transmission in the hippocampus, since more than fifty percent of the total AMPA/kainate receptor-mediated current received by CA3 pyramidal cells

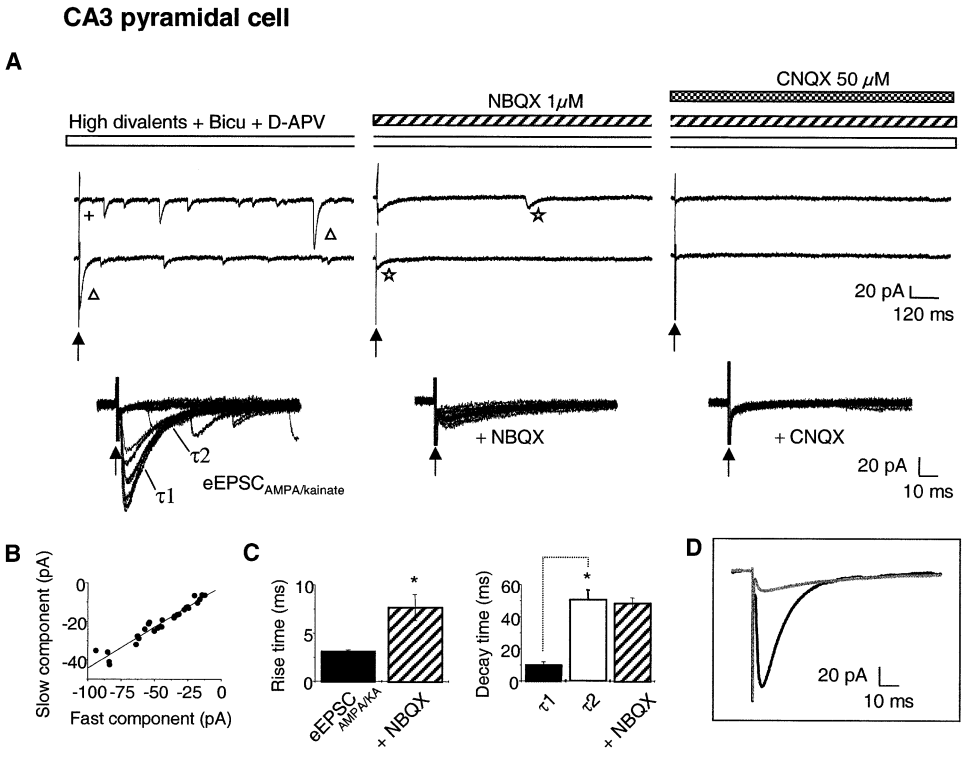

Figure 4. Unitary Mixed $EPSCs_{AMPA/kainate}$ Evoked by Minimal Stimulations in CA3 Pyramidal Cells

(A) The top shows representative recordings of spontaneous and minimally evoked EPSCs in a CA3 pyramidal cell in the presence of high-divalent ions (4 mM Ca^{2+}, 6 mM Mg^{2+}), bicuculline (10 μM), and D-APV (50 μM) to isolate AMPA/kainate receptor-mediated activity (Vh: −60 mV). In these conditions, minimal stimulation (arrow) with a glass electrode placed in stratum lucidum evokes either a double decaying $EPSC_{mixed}$ (open triangle symbol) or a transmission failure (+). The fast component of the $EPSC_{mixed}$ (tau 1) is mediated by AMPA receptors since it is blocked in the presence of NBQX (1 μM, middle); the slow component (tau 2) is mediated by kainate receptors since it is NBQX-resistant (open star symbol, middle) but CNQX-sensitive (right). Note that in both control (left) and NBQX (middle) conditions, sEPSCs with the same time course and amplitude as the evoked EPSC can be detected. The bottom shows superimposed traces of ten consecutively evoked EPSCs in the same pharmacological conditions as above (stimulation at arrow). Tau 1 and tau 2 indicate the first and second component of the mixed $EPSC_{AMPA/kainate}$.

(B) Plotted is the amplitude of the slow kainate receptor-mediated component versus the fast AMPA receptor-mediated component of the minimally evoked, double decaying EPSC. Note that there is a tight correlation between the amplitude of the AMPA and kainate receptor-mediated components ($r = 0.97$).

(C) Bar graph of averaged rise times (left) and decay times (right) of the values of minimally evoked EPSC in CA3 pyramidal cells ($n = 5$) show that the second component of the $EPSC_{mixed}$ has the same time course as the kainate receptor-mediated component.

(D) Superimposition of the digitally averaged, evoked EPSC shows that the second component of the $EPSC_{mixed}$ (black) perfectly fits the decay phase of the $EPSC_{kainate}$ evoked in the presence of NBQX (gray).

(53% ± 4.6%, $n = 25$) and CA1 interneurons (64% ± 3%, $n = 10$) was generated by kainate receptors (Figure 6).

Spontaneous $EPSC_{AMPA}$, Pure $EPSC_{kainate}$, and Mixed $EPSC_{AMPA/kainate}$ in CA3 Pyramidal Cells and CA1 Interneurons

To ensure that pure $EPSC_{AMPA}$, pure $EPSC_{kainate}$, and mixed $EPSC_{AMPA/kainate}$ could be observed in physiological conditions, spontaneous EPSCs (sEPSCs) were recorded in the absence of GABA, AMPA, and NMDA receptor antagonists. To isolate non-NMDA receptor-mediated events, spontaneous EPSCs were recorded at the reversal potential for GABAergic currents ($Vh = -70mV$). At this potential, the current mediated by NMDA receptors is nearly abolished by the Mg^{2+} block (Ascher and Nowak, 1988).

In CA3 pyramidal cells and CA1 interneurons, the population of non-NMDA sEPSCs was clearly heterogeneous since, in addition to fast sEPSCs, we observed events with a slow time course or a fall best fitted by a double exponential (Figure 7). The spontaneous fast, slow, and double decaying EPSCs had kinetics within the same range as that of $mEPSC_{AMPA}$, $mEPSC_{kainate}$, and $mEPSC_{AMPA/kainate}$, respectively (see Table 1 for values). As previously described for miniature EPSCs, part of these events were mediated by kainate receptors since they were resistant to the AMPA receptor antagonist GYKI 52466 (100 μM, $n = 5$; Figure 7), fully blocked by the mixed AMPA/kainate receptor antagonist CNQX (50 μM; data not shown) and had slow kinetics (r: 12.2 ± 0.6 ms, τ: 101.8 ± 1 ms in five CA3 pyramidal cells and r: 2.7 ± 0.05 ms, τ: 12.4 ± 0.6 ms in five CA1 interneurons), as compared to fast AMPA receptor-mediated events (Table 1). In CA1 pyramidal neurons, we observed a homogeneous population of fast EPSCs (Figure 7, Table 1) that were only mediated by AMPA receptors since they were fully blocked by the selective AMPA

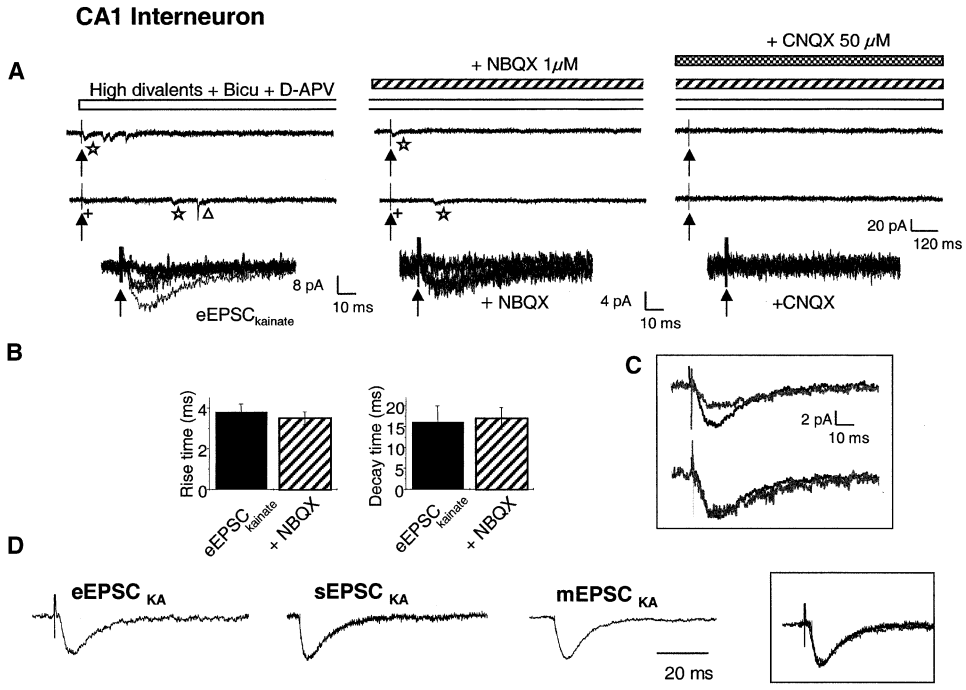

Figure 5. Unitary Pure $EPSCs_{kainate}$ Evoked by Minimal Stimulations in CA1 Stratum Oriens Interneurons

(A) The top shows representative recordings of spontaneous and minimally evoked EPSCs in a CA1 stratum oriens in the presence of high-divalent ions (4 mM Ca^{2+}, 6 mM Mg^{2+}), bicuculline (10 μM), and D-APV (50 μM) to isolate AMPA/kainate receptors-mediated activity (Vh: −60 mV). In these conditions, minimal stimulation (arrow) with a glass electrode placed close to the cell body evokes either a slowly decaying $EPSC_{kainate}$ (open star symbol) or a transmission failure (+); the evoked $EPSC_{kainate}$ is NBQX-resistant (open star symbol, middle) but CNQX-sensitive (right). Note that both in control (left) and NBQX (middle) conditions, sEPSCs with the same time course and amplitude as the evoked EPSC can be detected. The bottom shows superimposed traces of ten consecutively evoked EPSCs in the same pharmacological conditions as above (stimulation at arrow).

(B) A bar graph depicts averaged rise times (left) and decay times (right) values of minimally evoked EPSCs in CA1 interneurons (n = 4) showing that the time course of the minimally evoked $EPSC_{kainate}$ is unaltered in the presence of NBQX (1 μM).

(C) Superimposition of the digitally averaged, evoked EPSCs shows that NBQX (gray) decreases the amplitude (top), but does not alter the time course (bottom scaled traces), of the $EPSC_{kainate}$ evoked in control conditions (black).

(D) Evoked, spontaneous, and miniature $EPSC_{kainate}$ (digital averages) in a CA1 interneuron perfectly overlapped (superimposition in the insert) are shown.

receptor antagonist GYKI 52466 (100 μM, n = 5; Figure 7). Therefore, kainate receptors contribute to ongoing activity of hippocampal glutamatergic synapses in CA3 pyramidal cells and CA1 interneurons. The contribution of kainate receptors to spontaneous glutamatergic activity was difficult to estimate because of the frequent overlap of sEPSCs that precluded their identification. However, an estimation was possible in five stratum oriens interneurons that showed a low level of spontaneous glutamatergic activity. In these neurons, $sEPSC_{kainate}$ represented 31% ± 11% of the events, $sEPSC_{AMPA/kainate}$ 11% ± 3%, and $sEPSC_{AMPA}$ 57% ± 13% (n = 5).

Mixed $EPSC_{AMPA/kainate}$ Are Generated at Mossy Fiber Synapses onto CA3 Pyramidal Cells

The sources of glutamatergic innervation on CA3 pyramidal cells have been extensively defined as being opposed to those on stratum oriens interneurons. CA3 pyramidal cells receive glutamatergic inputs from three well-segregated major pathways: the mossy fiber pathway from dentate granular cells, the associational-commissural pathway from other CA3 pyramidal cells, and the perforant pathway from the entorhinal cortex. Among these pathways, several observations suggest that kainate receptors are specifically associated with mossy fibers (Ben Ari and Cossart, 2000; Castillo et al., 1997; Frerking and Nicoll, 2000; Lerma et al., 2001; Mulle et al., 1998; Represa et al., 1987). This hypothesis was tested using organotypic slice cultures (Stoppini et al., 1991). In this preparation, the mossy fibers can be eliminated by removal of the dentate gyrus and the consequences tested several days later. CA3 pyramidal cells were recorded after 7 days in culture to ensure the complete degeneration of the mossy fiber pathway (Qin et al., 2001). We relied on dynophin immunoreactivity, a selective marker of mossy fiber synapses (Henze et al., 1997), to establish the loss of mossy fibers and on αN-euN immunoreactivity to assess the absence of granular cells (Figure 8A). In control slice cultures (after 1 or 2 weeks in culture) $mEPSC_{AMPA}$ (r: 2.8 ± 0.26 ms and τ: 13.5 ± 1.4 ms, n = 11) and $mEPSC_{AMPA/kainate}$ (r: 2.7 ± 0.19 ms, τ1: 11 ± 1 ms, and τ2: 58.2 ± 7.2 ms, n = 11) were recorded at frequencies similar to those in acute slices. However, $mEPSC_{kainate}$ (r: 15 ± 2.2 ms and τ: 62.5 ± 24 ms) were less frequent than in acute slices (mean frequency: 0.01 ± 0.001 Hz, n = 11; $p < 0.05$; Figure 8),

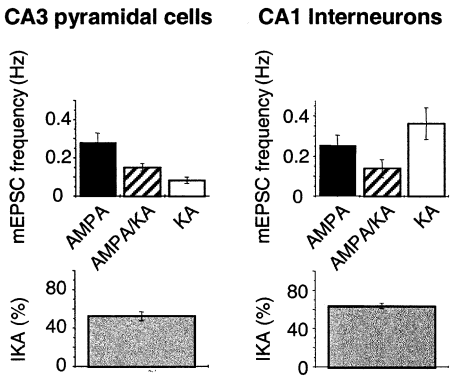

Figure 6. Contribution of Kainate Receptors to Miniature Glutamatergic Activity in CA3 Pyramidal Cells and CA1 Interneurons

The top depicts histograms of averaged frequencies of $mEPSC_{AMPA}$, $mEPSC_{AMPA/kainate}$, and $mEPSC_{kainate}$ in CA3 pyramidal cells (left, n = 25) and CA1 interneurons (right, n = 15). The bottom shows mean percentage of miniature current mediated by postsynaptic kainate receptors (see Experimental Procedures) in both cell types (n = 25 pyramidal cells and 15 interneurons).

possibly because of the lack of a synaptic input in the preparation, thus precluding a quantitative estimation of the source of the pure $EPSC_{kainate}$. In slices lacking the mossy fiber input pathway, only fast mEPSC (r: 2 ± 0.27 ms and τ: 10.2 ± 1.2 ms, mean frequency = 0.24 ± 0.08, n = 11) were detected in the presence of bicuculine (10 μM), D-APV(50 μM), and TTX (0.3–1 μM) (Figure 8B). These mEPSCs were fully blocked by the addition of NBQX (1 μM) or GYKI 52466 (100 μM; n = 11), showing that they were mediated by AMPA receptors. We conclude that the mixed $EPSC_{AMPA/kainate}$ are of mossy fiber origin. Further studies are required to determine the synaptic sources of the synaptic currents with a kainate components on CA1 interneurons.

Discussion

Our results show that kainate receptors can be activated by the quantal release of glutamate to generate pure unitary EPSCs or mixed unitary EPSCs when coactivated with AMPA receptors in the hippocampus. The relatively fast kinetics of pure kainate EPSCs in CA1 interneurons–not observed previously in central neurons–indicates that kainate receptors are localized in the synaptic cleft either with AMPA receptors or in pure kainate synapses. Furthermore, kainate receptors are major actors in the generation of ongoing basal glutamatergic synaptic transmission in the hippocampus: they provide as much as of half the total glutamatergic

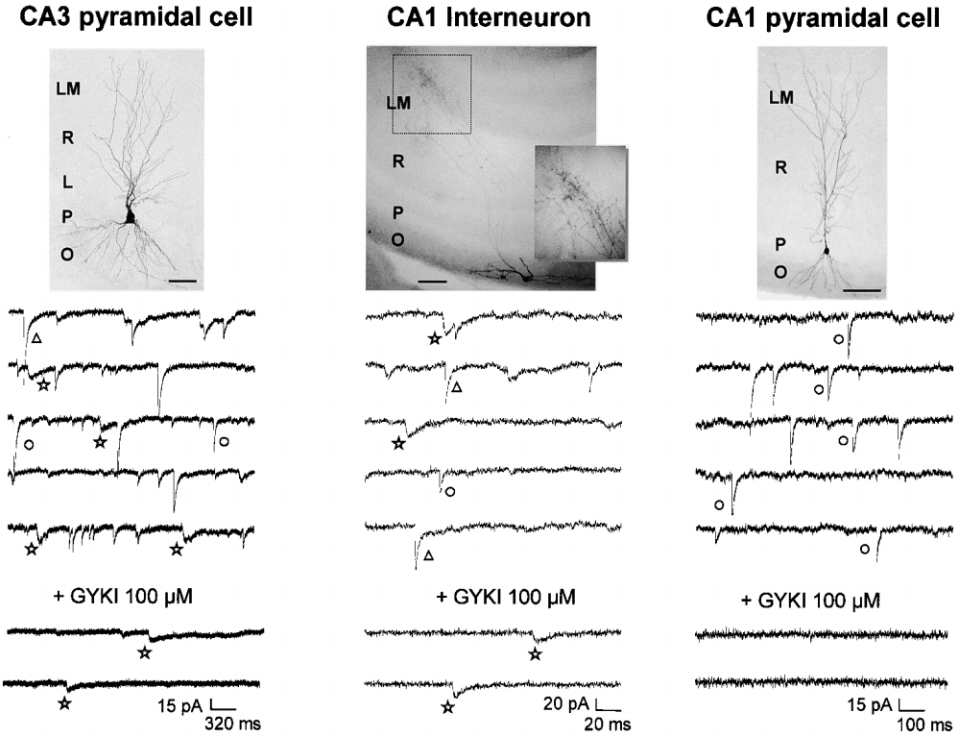

Figure 7. Kinetic Heterogeneity of Spontaneous EPSCs in CA1 Interneurons and CA3, But Not CA1, Pyramidal Cells

Representative sEPSCs recordings (Vh = −70 mV) from a CA3 pyramidal cell, a CA1 stratum oriens interneuron, and a CA1 pyramidal cell are shown. Note that in both the CA3 pyramidal cell and the CA1 interneuron, but not in the CA1 pyramidal neuron, three types of sEPSCs can be distinguished based on the time course of their decay: fast (open black circle), slow (open star symbol), and mixed EPSCs with a double decaying phase (open triangle symbol). Only events with slow kinetics remain in the presence of GYKI 52466 (100 μM, open star symbol, bottom traces). Photomicrographs (top) illustrate the biocytin-filled recorded neurons. The interneuron had a cell body in stratum oriens and an axon innervating stratum lacunosum moleculare (O-LM interneuron; see insert magnification 4×). Abbreviations: O, stratum oriens; P, stratum pyramidale; L, stratum lucidum; R, stratum radiatum; LM, stratum lacunosum moleculare.
Scale bar: 100 μm.

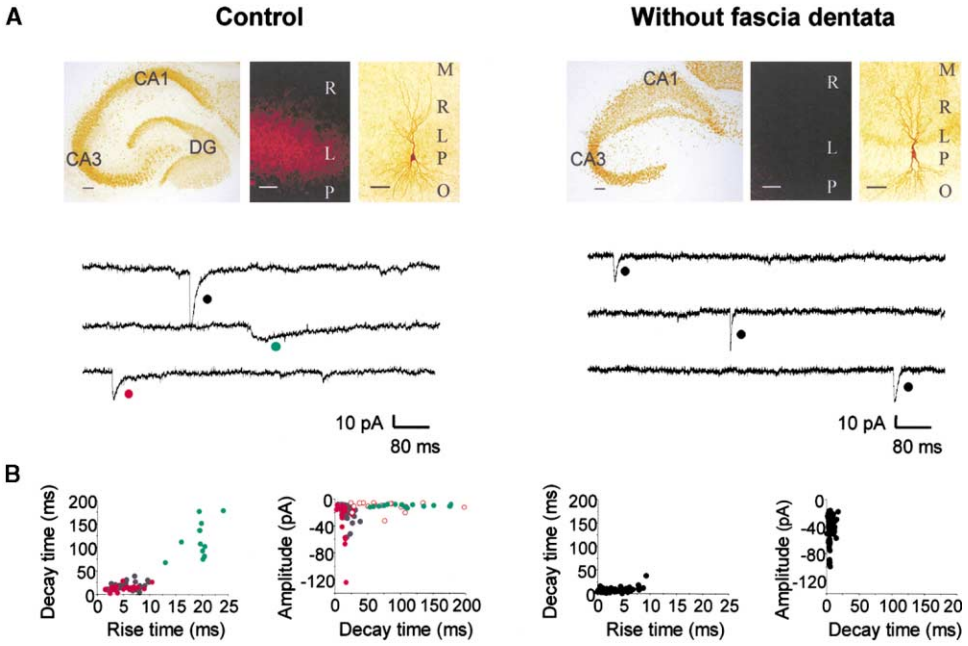

Figure 8. Mixed $EPSC_{AMPA/kainate}$ Are Generated in Mossy Fiber Synapses in CA3 Pyramidal Cells

(A) The top shows organotypic slice cultures control and after removal of fascia dentata, labeled with αNeuN (left) or dynorphin (middle) antibodies to selectively stain neuronal cell bodies and mossy fibbers terminals, respectively. Right photomicrograph illustrates CA3 biocytin-filled recorded pyramidal cells. Note that the absence of fascia dentata (assessed by the absence of staining with αNeuN antibody) was associated with a loss of mossy fiber terminals, which is depicted by the lack of dynorphin immunostaining. However, CA3 pyramidal cells displayed a normal morphology. The bottom illustrates miniature EPSCs recordings in the presence of TTX (1 μM), bicuculline (10 μM), and D-APV (50 μM) from a CA3 pyramidal cell in control organotypic slice culture (left) or culture lacking the fascia dentata (right). Note that in control conditions in this CA3 pyramidal cell, three types of mEPSCs can be distinguished based on the time course of their decay: fast (closed black circle), slow (closed green circle), and mixed EPSCs with a double decaying phase (closed red circle). Without the fascia dentata, only $mEPSC_{AMPA}$ (closed black circle) can be recorded.

(B) Scatter plots of the rise time constant (left column) or amplitude (right column) versus decay time constant calculated in mEPSCs recorded from a CA3 pyramidal cell in control organotypic slice cultures and in slice cultures lacking fascia dentata. Note that in control conditions, two families of events are clustered in separate areas of the graph are shown: the fast (closed black circle) and slow events (closed green circle). The decay time constant versus amplitude distributions obtained when plotting the first (closed red circle) and the second (open red circle) components of mixed events overlapped that of the fast (closed black circle) and slow event (closed green circle) families, respectively. In slice cultures lacking fascia dentata, only fast events (closed black circle) remained.

currents recorded in interneurons. Finally, our data provide direct evidence that, in CA3 pyramidal cells, AMPA and kainate receptors are most likely colocalized in individual mossy fiber synapses.

Pure $EPSC_{kainate}$ and Mixed $EPSC_{AMPA/kainate}$ in CA3 Pyramidal Cells and CA1 Stratum Oriens Interneurons

Relying on their pharmacological profile and kinetic properties, we have identified three types of miniature, spontaneous, and evoked glutamatergic currents in CA3 pyramidal cells and CA1 stratum oriens interneurons: pure $EPSC_{AMPA}$, mixed $EPSC_{AMPA/kainate}$, and pure $EPSC_{kainate}$. As expected, the fastest events were mediated by AMPA receptors ($EPSC_{AMPA}$), since they were fully blocked by AMPA receptor antagonists (GYKI and NBQX). In contrast, slow events were mediated by kainate receptors ($EPSC_{kainate}$), since they were resistant to AMPA receptor antagonists (GYKI and NBQX) and blocked by a selective antagonist for kainate receptors (SYM 2081) and a mixed AMPA/kainate receptor antagonist (CNQX). In addition, there is a population of events with a rapid rise time and a double exponential decay time that are generated by the coactivation of AMPA and kainate receptors ($EPSC_{AMPA/kainate}$) since: (1) the double decaying EPSCs are sensitive to both AMPA (GYKI and NBQX) and kainate (SYM2081) receptor antagonists and fully blocked by a mixed AMPA/kainate receptor antagonist (CNQX). (2) The averaged decay times of the first and second components of these events are identical to the averaged decay times of $mEPSC_{AMPA}$ and $mEPSC_{kainate}$, respectively. (3) The plots of amplitude versus decay time for the first and second component of these events are segregated in two regions of the graph that fully match the same plots obtained for $mEPSC_{AMPA}$ and $mEPSC_{kainate}$, respectively. (4) Minimal stimulation experiments show that the slow component of the evoked mixed EPSC is resistant to NBQX and fully blocked by CNQX. (5) The experiments using minimal stimulation suggest that the AMPA and kainate receptors mediating the evoked $EPSC_{AMPA/kainate}$ are likely to be located within the same synaptic cleft since there was a tight correlation between the amplitudes of AMPA and kainate receptors mediated components of the evoked EPSC (eEPSC) at each stimulation trial. Thus, in both CA3 pyramidal cells and CA1 interneurons, we can isolate

(in addition to the classically described fast $mEPSC_{AMPA}$) pure $mEPSC_{kainate}$ with a slower kinetics and mixed $mEPSC_{AMPA/kainate}$ with a fast rise time and a double decay.

Fast Kinetics of Unitary Kainate Receptor-Mediated Synaptic Currents in Interneurons

In our experiments, kainate receptor-mediated currents recorded in pure $EPSC_{kainate}$ and mixed $EPSC_{AMPA/kainate}$ were characterized by their slow time course and small amplitude when compared to AMPA receptor-mediated ones in CA1 interneurons and CA3 pyramidal cells. However, the time course of the kainate receptor-mediated current differed among cell types. In CA3 pyramidal cells, the decay time for kainate receptor-mediated currents ranged between 50 and 150 ms whereas in CA1 interneurons, it ranged between 5 and 15 ms.

Previous estimations of the decay kinetics of kainate receptor-mediated EPSCs relied primarily on values obtained by bulk stimulation protocols that ranged between 30 (Cossart et al., 1998; Li et al., 1999) and 100 (Castillo et al., 1997) ms. The pure spontaneous $EPSC_{kainate}$ recorded in developing cortical neurons also had a circa 200 ms decay time constant (Kidd and Isaac, 1999). To the best of our knowledge, EPSCs mediated by kainate receptors with a millisecond decay time constant have only been reported in "off" bipolar cells (DeVries, 2000). Considering the time course of $EPSC_{kainate}$ in CA1 interneurons, we now show that in the hippocampus as in the retina, synaptic kainate receptor-mediated currents have a time course as fast as that measured upon glutamate application for heterologously expressed kainate receptors (Cui and Mayer, 1999; Swanson and Heinemann, 1998). Therefore, at least in interneurons, the kinetics of kainate receptor-mediated currents is most likely due to intrinsic properties of kainate receptors rather than to the diffusion of glutamate or other factors (see Frerking and Nicoll, 2000, and Lerma et al., 2001, for a review). In contrast, in CA3 pyramidal cells, the kinetics of $EPSC_{kainate}$ is slower than in CA1 interneurons and heterologous expression systems but is similar to that of the evoked $EPSC_{kainate}$ (Castillo et al., 1997; Vignes and Collingridge, 1997). The origin of such difference could be the synaptic kainate receptor subunit composition (Cossart et al., 1998; Cui and Mayer, 1999; Mulle et al., 1998, 2000), intracellular signals, or accessory proteins (Garcia et al., 1998). Another hypothesis is that this difference could be due to the architectonic properties of CA3 pyramidal cells, such as the size of the cells, the number of neurites, and the proportion of dendritic spines that have been shown to alter the time course of synaptic events (Livsey and Vicini, 1992). In keeping with this, the $EPSC_{AMPA}$ is also twice as slow in CA3 than in CA1 pyramidal cells (Table 1). Future studies will have to explain these differences.

Another characteristic property of kainate receptor-mediated currents is their small amplitude relative to AMPA receptor-mediated currents (Frerking and Nicoll, 2000; Lerma et al., 2001). This is particularly clear in mixed $EPSC_{AMPA/kainate}$, as shown by the plots of mEPSCs amplitude versus decay time constant. Thus, the small peak amplitude of kainate receptor-mediated currents seems to be a general property. This could be due to a small number of kainate receptors opened at the peak of the EPSC (Frerking et al., 1998) to a smaller, single-channel conductance (Swanson et al., 1996) or to different properties of glutamate-releasing sites. However, the latter explanation is unlikely, since in unitary mixed $EPSC_{AMPA/kainate}$, the amplitude of the kainate component is always smaller than the AMPA one. Nevertheless, it is important to emphasize that in spite of their small amplitude, the charge carried by kainate receptor-mediated currents is greater in CA3 pyramidal cells and CA1 interneurons than that of AMPA receptors due to their slower time course.

Kainate Receptors Provide a Substantial Proportion of the EPSCs Recorded in CA3 Pyramidal Cells and CA1 Stratum Oriens Interneurons

We estimated the contribution of kainate receptors to basal glutamatergic activity in two ways: first, as the proportion of events involving the activation of kainate receptors and second, as the percentage of current resulting from their activation. Our analysis relied on the kinetics of the three types of events in physiological conditions (i.e., without blockers). One important condition to validate this conclusion is to preclude the possibility that because of inadequate clamp conditions–particularly at distal dendritic sites–some small $EPSC_{kainate}$ would be, in fact, filtered $EPSC_{AMPA}$. The following observations cannot be reconciled with this possibility. (1) In CA1 pyramidal neurons that are devoid of kainate receptors and where EPSCs are mediated only by AMPA receptors, despite the presence of distally generated $EPSC_{AMPA}$, there were no events with as slow kinetics as $EPSC_{kainate}$. (2) Single exponential fast AMPA and slow events were clustered in two separate regions of the graphs plotting mEPSCs rise times versus decay times. Similar plots of distally and locally generated events mediated by the same receptor type do not cluster in two discrete regions but, rather, tend to form a continuum (Bekkers and Stevens, 1996). (3) The slowest $mEPSC_{AMPA}$–recorded when kainate receptors were blocked by SYM–were still faster than the kinetics of the fastest $mEPSC_{kainate}$ recorded in GYKI. This enabled us to define a "kinetic threshold" to identify kainate receptor-mediated events. (4) The charge underlying each EPSC, a parameter classically considered not to be affected by electrotonic filtering (Bekkers and Stevens, 1996; Magee and Cook, 2000), was significantly different between $EPSC_{AMPA}$ and the $EPSC_{kainate}$. (5) Selective lesion of the mossy fibers eliminates the slow component of the mixed $EPSC_{AMPA/kainate}$ without affecting pure $EPSC_{AMPA}$. This is important as the mossy fiber synapses are close to the cell body, and the voltage clamp conditions have been shown to be adequate for that synapse (Henze et al., 1997). Our estimation of the contribution of the $EPSC_{AMPA/kainate}$ could be biased because of a chance probability that pure fast and slow events coincide to generate a mixed event. However, this can be excluded because the frequency of the pure $EPSC_{kainate}$ is lower in CA3 pyramidal neurons than the mixed $EPSC_{AMPA/kainate}$. Also, the frequency of miniatures $EPSC_{AMPA}$ and $EPSC_{kainate}$ is very low and the likelihood that two events coincide during an EPSC is negligible; in keeping with this, we never detected a mixed event beginning with an $EPSC_{kainate}$. Finally, this possibility can-

not be reconciled with the loss of the $EPSC_{AMPA/kainate}$ following lesions of the mossy fibers.

Frequency analysis of the three types of miniature events revealed that around 45% of miniature events involved kainate receptors in CA3 pyramidal cells and 65% in CA1 interneurons. Taking into account the frequency of each type of event and the charge carried respectively by AMPA and kainate receptor-mediated currents, we estimated that in our experimental conditions, half of the glutamatergic current is generated by activation of kainate receptors in CA3 pyramidal cells and CA1 interneurons. Therefore, we conclude that in cells that express functional postsynaptic kainate receptors, these receptors substantially participate in basal glutamatergic activity. These results are quite unexpected since previous reports have shown that kainate receptor-mediated responses were difficult to detect (Frerking and Nicoll, 2000). However, it is important to stress that in these studies, the kainate receptor-mediated responses were isolated in the presence of the AMPA receptor antagonist GYKI, a drug that also blocks more than half of the kainate response (Frerking et al., 1998, and present data).

Since each type of unitary EPSC had a very characteristic kinetic signature (Table 1), we were also able to isolate spontaneous $EPSC_{kainate}$ and $EPSC_{AMPA/kainate}$ in physiological conditions. The three types of events ($sEPSC_{AMPA}$, $sEPSC_{kainate}$, and $sEPSC_{AMPA/kainate}$) were present in the spontaneous glutamatergic activity of CA3 pyramidal cells and CA1 interneurons. However, we could not measure the respective frequency of each type of event due to the high level of glutamatergic activity in the absence of TTX. Nevertheless, our results show that kainate receptors provide a substantial proportion of the glutamatergic currents in adult hippocampal neurons. Thus, the participation of these receptors is not restricted to immature neurons, as suggested on the basis of responses evoked by bulk stimulation in the thalamo-cortical system (Kidd and Isaac, 1999).

$EPSC_{AMPA/kainate}$ in CA3 Pyramidal Cells Are Generated at Mossy Fiber Synapses

The presence of $EPSC_{AMPA}$, $EPSC_{kainate}$, and mixed $EPSC_{AMPA/kainate}$ in the hippocampus (with different temporal signatures) adds to the diversity of glutamatergic synaptic transmission. Since the hippocampus integrates information from different structures, this diversity could enable neurons to discriminate between these inputs, as in the retina (DeVries, 2000). In this case, it must be possible to assign to each type of event a specific presynaptic source. Kainate receptors expressed on CA3 pyramidal cells are classically associated to the mossy fiber pathway (Represa et al., 1987; Castillo et al., 1997; Petralia et al., 1994). The selective elimination of mixed $EPSC_{AMPA/kainate}$ by the removal of granule cells from organotypic slices provides direct evidence that these events are indeed generated at mossy fiber synapses. Future studies are required to identify the sources of the pure $EPSC_{kainate}$, in particular in interneurons, considering their clearly major role in glutamatergic transmission in these cells. It will be also interesting to determine whether the three types of EPSCs are differentially affected, in particular in relation to the epilepsies in which hippocampal kainate receptors play an important role (Ben-Ari, 1985; Ben-Ari and Cossart, 2000).

In conclusion, our results indicate that in the hippocampus, there is a highly significant and diversified contribution of kainate receptors to glutamatergic synaptic transmission. Clearly, glutamatergic synapses are mediated by both AMPA and kainate receptors in ongoing conditions of activation, in addition to NMDA receptors that will also be activated in more depolarised conditions. Interestingly, the two cell types in which kainate receptors contribute to basal glutamatergic neurotransmission (i.e., CA3 pyramidal cells and CA1 interneurons) are critically involved in the generation and control of rhythmic activities (McBain and Fisahn, 2001; Miles and Wong, 1983). Therefore, kainate receptor-mediated events, with their relatively slow kinetics (as compared to $EPSC_{AMPA}$), might play an important role in synchronizing the network through the temporal summation of afferent inputs. Because the kinetics of kainate receptor-mediated currents is faster in interneurons than in pyramidal cells, the frequency pattern of afferent synaptic activity necessary for temporal summation should be faster in interneurons than in pyramidal cells (Traub et al., 2000).

Experimental Procedures

Electrophysiology

Transverse hippocampal slices (400 μm thick) were obtained from 12- to 21-day-old male Wistar rats. Rats were decapitated under deep anesthesia with chloral hydrate (i.p., 350 mg/kg) and hippocampal slices were cut using a chopper (McIlwain, U.S.A.) or a Leica VT1000S tissue slicer. Slices were superfused continuously with artificial cerebrospinal fluid (ACSF) containing 126 mM NaCl, 3.5 mM KCl, 1.2 mM NaH_2PO_4, 26 mM $NaHCO_3$, 1.3 mM $MgCl_2$, 2 mM $CaCl_2$, 10 mM D-glucose and aerated with 95% O_2 and 5% CO_2.

After rest (>1 hr), slices were individually transferred to a recording chamber maintained at 30°–32°C and continuously perfused with oxygenated ACSF. Whole-cell recordings of spontaneous and miniature glutamatergic postsynaptic currents (PSCs) were obtained using tight-seal electrodes (3–10 MΩ) filled with an internal solution containing: 135 mM Cs-gluconate, 10 mM $MgCl_2$, 0.1 mM $CaCl_2$, 1 mM EGTA, 10 mM HEPES, 0.5% biocytin (pH 7.25), complemented in some experiments with 2 mM MgATP and 0.4 mM NaGTP. No differences were observed between both internal solutions.

The pyramidal cell layer was visualized with a binocular magnifying glass (Leica MZ6), while interneurons were visually identified with an IR-DIC microscope (Leica DM LFS) through a 40× water immersion objective. During recordings, neurons were filled passively with biocytin for post hoc identification (see Morphology). Miniature recordings were performed at −60 mV and spontaneous recordings at the reversal potential for GABAergic PSCs (−70 mV). Minimal stimulations were performed via a glass electrode filled with saline placed near the cell body (CA3 stratum lucidum or CA1 stratum oriens). The stimulus intensity and duration were adjusted to observe failures of synaptic transmission (between 40–80 μA and 20–30 μs).

Signals were fed to an EPC9 (HEKA, Heidelberg, Germany) or an Axopatch 2B amplifier (Axon Instruments, USA), filtered (2 kHz), digitized (10 kHz) with a Labmaster interface card (Axon Instruments) to a personal computer, and analyzed with MiniAnalysis 5.1 program (Synaptosoft, USA). Access resistance ranged between 10–20 MΩ, and the results were discarded if it changed by more than 20%.

Analysis

Each single event in each recorded cell was fully characterized by the following parameters: rise time (10%–90%), amplitude, and decay time constants were calculated using MiniAnalysis 5.1. The

baseline noise ranged between 3–5 pA, and an amplitude threshold of 2 pA more than the baseline noise was used for event detection. The false positive and false negative events represented less than 5% of the total events. To discriminate between each category of events in the absence of AMPA or kainate receptor antagonists, the following procedure was followed: all the events of each cell were individually fitted using the MiniAnalysis program 5.1. First, the mixed AMPA/kainate receptor-mediated events were identified as events with a decay time constant best fitted by a double exponential. The standard deviation given by the fit was used to determine whether one or two exponentials best fitted the decays. Then, to separate the mono exponentially fitted fast AMPA from the slow kainate receptor-mediated events, a "kinetic limit" was determined. The mono exponential decay times versus rise times were plotted for all the events in each cell. From this graph (in which fast AMPA and slow kainate receptor-mediated events were completely segregated in two distinct areas), the kinetic limit was determined. Using this method, we observed that fast AMPA and slow kainate receptor-mediated events could be easily differentiated on the basis of their decay time, as previously described (Kidd and Isaac, 1999). The limit of the decay time to separate fast AMPA and slow kainate receptor-mediated events was around 50 ms for CA3 pyramidal cells (i.e., events with a decay time slower than 50 ms were considered as kainate receptor-mediated) and 5 ms for CA1 interneurons.

The charge transfer through the AMPA and kainate receptor-mediated EPSCs ($Q_{AMPA}[EPSC_{AMPA}]$ and $Q_{kainate}[EPSC_{kainate}]$, respectively) was given by the area underlying the digitally averaged traces. The charge transfer through the AMPA and kainate receptor-mediated components of the dual component $EPSC_{AMPA/kainate}$ ($Q_{AMPA}[EPSC_{AMPA/kainate}]$ and $Q_{kainate}[EPSC_{AMPA/kainate}]$, respectively) were estimated by calculating the product of the decay and the current at peak obtained from the exponential fits. The current mediated by AMPA or kainate receptor was the product of the total charge carried by AMPA or kainate receptor-mediated currents in each event type and the frequency of each event type: $I_{AMPA} = Q_{AMPA}[EPSC_{AMPA}] \times f[EPSC_{AMPA}] + Q_{AMPA}[EPSC_{AMPA/kainate}] \times f[EPSC_{AMPA/kainate}]$ $I_{kainate} = Q_{KA}[EPSC_{kainate}] \times f[EPSC_{kainate}] + Q_{kainate}[EPSC_{AMPA/kainate}] \times f[EPSC_{AMPA/kainate}]$. All the experimental values are given as means ± SEM. Student's t test was used for statistical comparisons except when otherwise indicated ($p < 0.05$ was considered significant).

Organotypic Slice Culture

Procedure

Organotypic slices were prepared from hippocampi on postnatal day (P)10 male Wistar rats, according to the procedure described by Stoppini et al. (1991) with minor changes. Briefly, rats were decapitated under deep anesthesia with chloral hydrate (i.p., 350 mg/kg). All the next steps were performed under a laminar flow hood, using sterile techniques. Following the removal of the brain, the hippocampi were isolated, and hippocampal sections 400 μm thick were prepared using a chopper (McIlwain, USA) and collected in a PBS solution supplemented with 0.5% D-glucose. To obtain lesioned slices, the dentate gyrus was surgically removed under a binocular glass. Slices were kept at 4°C for 30 min in PBS-glucose and then placed onto Millicell-CM culture inserts (0.4 μm; Millipore; three slices per insert). The inserts were placed into six-well culture plates with 1 ml medium of the following composition: MEM (Sigma) supplemented with: 25 mM Glucose, 30 mM HEPES, 5 mM Na_2CO_3, 3 mM L-Glutamine, 0.5 mM L-Ascorbic Acid, 2 mM $CaCl_2H_2$, 2.5 mM $MgSO_4$, and 1 mg/l insulin (pH 7.25–7.29 with horse serum [20%]). Slices were maintained for 1–2 weeks in a cell culture incubator at 37°C in an atmosphere containing 5% $C0_2$. This was done to ensure a complete degeneration of the mossy fibers following removal of the fascia dentata. The medium was changed three times per week.

Immunocytochemistry

Organotypic slices were fixed by immersion for 1 hr at room temperature in 4% paraformaldehyde in PBS and incubated for 30 min in methanol containing 0.4% H_2O_2. After rinsing and a 30 min incubation in 2% normal goat serum in PBS containing 0.3% Triton X-100, the tissues were incubated overnight at 4°C with the monoclonal primary antibody αNeuN (1:10,000, Sigma) or the polyclonal antidynorphin (1:5000, Penynsula) in the same solution. Antigen-antibody complex were revealed using the avidin-biotin-peroxydase procedure (ABC, Vectastain Elite; Vector Labs).

Morphology

Slices were fixed overnight at 4°C in a solution containing 4% paraformaldehyde in 0.1 M phosphate buffer (PB) (pH 7.4). After fixation, slices were rinsed in PBS, cryoprotected in sucrose, and quickly frozen on dry ice. To neutralize endogenous peroxidase, slices were pretreated for 30 min in 1% H_2O_2. After several rinses in saline phosphate buffer (0.1 M PBS) (pH 7.4), slices were incubated for 24 hr at room temperature in 1:100 avidin-biotinylated peroxidase complex (Vector Laboratories, Inc., Burlingame, CA) diluted in PBS containing 0.3% Triton X-100. After 30 min rinses in PBS, slices were processed with 0.06% 3,3′-diaminobenzidine tetrahydrochloride (DAB, Sigma, St. Louis, MO) and 0.006% H_2O_2 diluted in PBS.

Chemicals

CNQX, D-APV, GYKI 52466, NBQX, and biocytin were obtained from Sigma, TTX from Latoxan, and SYM 2081 from Fisher Bioblock. GYKI 53655 was kindly provided by Dr. Leander (Lilly Research Centre, Ltd.). All of the compounds used for organotypic slice cultures were purchased from Sigma.

Acknowledgments

We thank I. Jorquera and N. Ferrand for technical assistance and Drs. A. Represa, C. Bernard, R. Khazipov, J.-L. Gaïarsa, and L. Aniksztejn for helpful comments. R.C. is supported by a grant of the French Ligue against Epilepsy and R.T. by the Fondation pour la Recherche Médicale (FRM). Financial support is also acknowledged from the FRM.

Received: October 19, 2001
Revised: May 29, 2002

References

Ascher, P., and Nowak, L. (1988). The role of divalent cations in the N-methyl-D-aspartate responses of mouse central neurones in culture. J.Physiol. (Lond.) *399*, 247–266.

Bekkers, J.M., and Stevens, C.F. (1996). Cable properties of cultured hippocampal neurons determined from sucrose-evoked miniature EPSCs. J. Neurophysiol. *75*, 1250–1255.

Ben-Ari, Y. (1985). Limbic seizure and brain damage produced by kainic acid: mechanisms and relevance to human temporal lobe epilepsy. Neuroscience *14*, 375–403.

Ben-Ari, Y., and Cossart, R. (2000). Kainate, a double agent that generates seizures: two decades of progress. Trends Neurosci. *23*, 580–587.

Bureau, I., Bischoff, S., Heinemann, S.F., and Mulle, C. (1999). Kainate receptor-mediated responses in the CA1 field of wild-type and GluR6-deficient mice. J.Neurosci. *19*, 653–663.

Bureau, I., Dieudonne, S., Coussen, F., and Mulle, C. (2000). Kainate receptor-mediated synaptic currents in cerebellar Golgi cells are not shaped by diffusion of glutamate. Proc. Natl. Acad. Sci. USA *97*, 6838–6843.

Castillo, P.E., Malenka, R.C., and Nicoll, R.A. (1997). Kainate receptors mediate a slow postsynaptic current in hippocampal CA3 neurons. Nature *388*, 182–186.

Cossart, R., Esclapez, M., Hirsch, J.C., Bernard, C., and Ben-Ari, Y. (1998). GluR5 kainate receptor activation in interneurons increases tonic inhibition of pyramidal cells. Nat. Neurosci. *1*, 470–478.

Cui, C., and Mayer, M.L. (1999). Heteromeric kainate receptors formed by the coassembly of GluR5, GluR6, and GluR7. J. Neurosci. *19*, 8281–8291.

DeVries, S.H. (2000). Bipolar cells use kainate and AMPA receptors to filter visual information into separate channels. Neuron *28*, 847–856.

Frerking, M., and Nicoll, R.A. (2000). Synaptic kainate receptors. Curr. Opin. Neurobiol. *10*, 342–351.

Frerking, M., Malenka, R.C., and Nicoll, R.A. (1998). Synaptic activation of kainate receptors on hippocampal interneurons. Nat. Neurosci. *1*, 479–486.

Garcia, E.P., Mehta, S., Blair, L.A., Wells, D.G., Shang, J., Fukushima,

T., Fallon, J.R., Garner, C.C., and Marshall, J. (1998). SAP90 binds and clusters kainate receptors causing incomplete desensitization. Neuron *21*, 727–739.

Henze, D.A., Card, J.P., Barrionuevo, G., and Ben-Ari, Y. (1997). Large amplitude miniature excitatory postsynaptic currents in hippocampal CA3 pyramidal neurons are of mossy fiber origin. J. Neurophysiol. *77*, 1075–1086.

Katona, I., Acsady, L., and Freund, T.F. (1999). Postsynaptic targets of somatostatin-immunoreactive interneurons in the rat hippocampus. Neuroscience *88*, 37–55.

Kidd, F.L., and Isaac, J.T. (1999). Developmental and activity-dependent regulation of kainate receptors at thalamocortical synapses. Nature *400*, 569–573.

Lerma, J., Paternain, A.V., Rodriguez-Moreno, A., and Lopez-Garcia, J.C. (2001). Molecular physiology of kainate receptors. Physiol. Rev. *81*, 971–998.

Li, H., and Rogawski, M.A. (1998). GluR5 kainate receptor mediated synaptic transmission in rat basolateral amygdala in vitro. Neuropharmacology *37*, 1279–1286.

Li, P., Wilding, T.J., Kim, S.J., Calejesan, A.A., Huettner, J.E., and Zhuo, M. (1999). Kainate-receptor-mediated sensory synaptic transmission in mammalian spinal cord. Nature *397*, 161–164.

Livsey, C.T., and Vicini, S. (1992). Slower spontaneous excitatory postsynaptic currents in spiny versus aspiny hilar neurons. Neuron *8*, 745–755.

Magee, J.C., and Cook, E.P. (2000). Somatic EPSP amplitude is independent of synapse location in hippocampal pyramidal neurons. Nat. Neurosci. *3*, 895–903.

McAllister, A.K., and Stevens, C.F. (2000). Nonsaturation of AMPA and NMDA receptors at hippocampal synapses. Proc. Natl. Acad. Sci. USA *97*, 6173–6178.

McBain, C.J., and Fisahn, A. (2001). Interneurons unbound. Nat. Rev. Neurosci. *2*, 11–23.

Miles, R., and Wong, R.K. (1983). Single neurones can initiate synchronized population discharge in the hippocampus. Nature *306*, 371–373.

Mulle, C., Sailer, A., Perez-Otano, I., Dickinson-Anson, H., Castillo, P.E., Bureau, I., Maron, C., Gage, F.H., Mann, J.R., Bettler, B., and Heinemann, S.F. (1998). Altered synaptic physiology and reduced susceptibility to kainate-induced seizures in GluR6-deficient mice. Nature *392*, 601–605.

Mulle, C., Sailer, A., Swanson, G.T., Brana, C., O'Gorman, S., Bettler, B., and Heinemann, S.F. (2000). Subunit composition of kainate receptors in hippocampal interneurons. Neuron *28*, 475–484.

Paternain, A.V., Morales, M., and Lerma, J. (1995). Selective antagonism of AMPA receptors unmasks kainate receptor-mediated responses in hippocampal neurons. Neuron *14*, 185–189.

Petralia, R.S., Wang, Y.X., and Wenthold, R.J. (1994). Histological and ultrastructural localization of the kainate receptor subunits, KA2 and GluR6/7, in the rat nervous system using selective antipeptide antibodies. J. Comp. Neurol. *349*, 85–110.

Qin, L., Marrs, G.S., McKim, R., and Dailey, M.E. (2001). Hippocampal mossy fibers induce assembly and clustering of PSD95-containing postsynaptic densities independent of glutamate receptor activation. J. Comp. Neurol. *440*, 284–298.

Represa, A., Tremblay, E., and Ben-Ari, Y. (1987). Kainate binding sites in the hippocampal mossy fibers: localization and plasticity. Neuroscience *20*, 739–748.

Stoppini, L., Buchs, P.A., and Muller, D. (1991). A simple method for organotypic cultures of nervous tissue. J. Neurosci. Methods *37*, 173–182.

Swanson, G.T., and Heinemann, S.F. (1998). Heterogeneity of homomeric GluR5 kainate receptor desensitization expressed in HEK293 cells. J. Physiol. (Lond.) *513*, 639–646.

Swanson, G.T., Feldmeyer, D., Kaneda, M., and Cull-Candy, S.G. (1996). Effect of RNA editing and subunit co-assembly single-channel properties of recombinant kainate receptors. J. Physiol. (Lond.) *492*, 129–142.

Traub, R.D., Bibbig, A., Fisahn, A., LeBeau, F.E., Whittington, M.A., and Buhl, E.H. (2000). A model of gamma-frequency network oscillations induced in the rat CA3 region by carbachol in vitro. Eur. J. Neurosci. *12*, 4093–4106.

Vignes, M., and Collingridge, G.L. (1997). The synaptic activation of kainate receptors. Nature *388*, 179–182.

Watt, A.J., van Rossum, M.C., MacLeod, K.M., Nelson, S.B., and Turrigiano, G.G. (2000). Activity coregulates quantal AMPA and NMDA currents at neocortical synapses. Neuron *26*, 659–670.

Wilding, T.J., and Huettner, J.E. (1995). Differential antagonism of alpha-amino-3-hydroxy-5-methyl-4- isoxazolepropionic acid-preferring and kainate-preferring receptors by 2,3-benzodiazepines. Mol. Pharmacol. *47*, 582–587.